



HAL
open science

Ground-based and satellite observations of high-latitude auroral activity in the dusk sector of the auroral oval

K. Kauristie, T. I. Pulkkinen, O. Amm, A. Viljanen, M. Syrjäso, P. Janhunen, S. Massetti, S. Orsini, M. Candidi, J. Watermann, et al.

► **To cite this version:**

K. Kauristie, T. I. Pulkkinen, O. Amm, A. Viljanen, M. Syrjäso, et al.. Ground-based and satellite observations of high-latitude auroral activity in the dusk sector of the auroral oval. *Annales Geophysicae*, 2001, 19 (10/12), pp.1683-1696. hal-00316959

HAL Id: hal-00316959

<https://hal.science/hal-00316959>

Submitted on 18 Jun 2008

HAL is a multi-disciplinary open access archive for the deposit and dissemination of scientific research documents, whether they are published or not. The documents may come from teaching and research institutions in France or abroad, or from public or private research centers.

L'archive ouverte pluridisciplinaire **HAL**, est destinée au dépôt et à la diffusion de documents scientifiques de niveau recherche, publiés ou non, émanant des établissements d'enseignement et de recherche français ou étrangers, des laboratoires publics ou privés.

Ground-based and satellite observations of high-latitude auroral activity in the dusk sector of the auroral oval

K. Kauristie¹, T. I. Pulkkinen¹, O. Amm¹, A. Viljanen¹, M. Syrjäso¹, P. Janhunen¹, S. Massetti², S. Orsini², M. Candidi², J. Watermann³, E. Donovan⁴, P. Prikryl⁵, I. R. Mann⁶, P. Eglitis⁷, C. Smith⁸, W. F. Denig⁹, H. J. Opgenoorth^{1,7}, M. Lockwood¹⁰, M. Dunlop¹¹, A. Vaivads⁷, and M. André⁷

¹Finnish Meteorological Institute, Geophysical Research Division, P.O.Box 503, FIN-00101 Helsinki, Finland

²Consiglio Nazionale delle Ricerche, Istituto di Fisica dello Spazio Interplanetario, Rome, Italy

³Danish Meteorological Institute, Solar-Terrestrial Physics Division, Copenhagen, Denmark

⁴University of Calgary, Department of Physics and Astronomy, Alberta, Canada

⁵Communications Research Centre, Ottawa, Canada

⁶University of York, Department of Physics, UK

⁷Swedish Institute of Space Physics, Uppsala Division, Sweden

⁸Bartol Research Institute, Delaware, USA

⁹Air Force Research Laboratory, Hanscom Air Force Base, Massachusetts, USA

¹⁰Rutherford Appleton Laboratory, Didcot, UK

¹¹Imperial College, London, UK

Received: 25 April 2001 – Revised: 21 June 2001 – Accepted: 23 June 2001

Abstract. On 7 December 2000, during 13:30–15:30 UT the MIRACLE all-sky camera at Ny Ålesund observed auroras at high-latitudes (MLAT ~ 76) simultaneously when the Cluster spacecraft were skimming the magnetopause in the same MLT sector (at $\sim 16:00$ – $18:00$ MLT). The location of the auroras (near the ionospheric convection reversal boundary) and the clear correlation between their dynamics and IMF variations suggests their close relationship with R1 currents. Consequently, we can assume that the Cluster spacecraft were making observations in the magnetospheric region associated with the auroras, although exact magnetic conjugacy between the ground-based and satellite observations did not exist. The solar wind variations appeared to control both the behaviour of the auroras and the magnetopause dynamics. Auroral structures were observed at Ny Ålesund especially during periods of negative IMF B_Z . In addition, the Cluster spacecraft experienced periodic ($T \sim 4 - 6$ min) encounters between magnetospheric and magnetosheath plasmas. These undulations of the boundary can be interpreted as a consequence of tailward propagating magnetopause surface waves. Simultaneous dusk sector ground-based observations show weak, but discernible magnetic pulsations (Pc 5) and occasionally periodic variations ($T \sim 2 - 3$ min) in the high-latitude auroras. In the dusk sector, Pc 5 activity was stronger and had characteristics that were consistent with a field line resonance type of activity. When IMF B_Z stayed positive for a longer period, the auroras were dimmer and the spacecraft stayed at the outer edge of the magnetopause where they observed electromagnetic pulsations

with $T \sim 1$ min. We find these observations interesting especially from the viewpoint of previously presented studies relating poleward-moving high-latitude auroras with pulsation activity and MHD waves propagating at the magnetospheric boundary layers.

Key words. Ionosphere (ionosphere-magnetosphere interaction) – Magnetospheric physics (auroral phenomena; solar wind – magnetosphere interactions)

1 Introduction

Auroral activity is frequently observed in the post-noon and dusk sectors of the auroral oval. All-sky cameras (ASC) at high-latitude stations observe multiple discrete auroral arcs with longitudinally propagating brightenings, folds, or spirals. These auroras can occasionally be bright but usually they are dimmer and more transient than for example, a growth phase aurora in the pre-midnight sector.

If the dusk component of the interplanetary magnetic field (IMF B_Y) is strongly positive, then the northern hemispheric cusp region can shift from the noon to dusk sector as a consequence of the partial penetration of the IMF to the magnetospheric cavity (Cowley et al., 1991). Under IMF $B_Y > 0$ conditions, the region favouring reconnection of the IMF and magnetospheric field lines at the dayside magnetopause shifts duskwards (Luhmann et al., 1984). Consequently, reconnection-related auroras which typically appear in the noon sector can be observed also in the afternoon and dusk sectors (Moen et al., 1999). One such example is

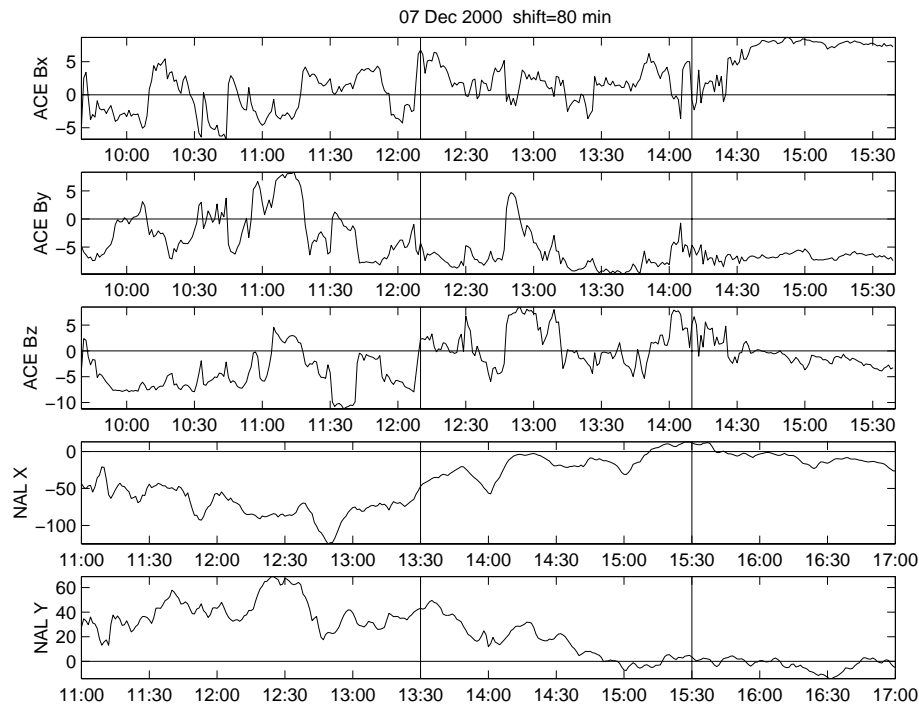


Fig. 1. IMF B_X , B_Y , and B_Z (GSE-coordinates) by the ACE satellite (three first panels) and magnetic field north and east components as recorded at Ny Ålesund (NAL). The vertical lines show the period of auroral activity at NAL.

analysed in this issue by Opgenoorth et al. (2001). If the north component of the IMF (IMF B_Z) is negative, then cusp auroras are related to so-called flux transfer events (FTEs) with specific ground magnetic (McHenry and Clauer, 1987) and ionospheric plasma flow (Provan et al., 1998) signatures and velocity dispersed ion signatures in the low-altitude particle precipitation data (Lockwood et al., 1996). The auroras appear typically at the poleward boundary of the auroral oval where they propagate poleward (and also westward if IMF $B_Y > 0$) into the polar cap. Auroral activity occurs quasi-periodically with a recurrence rate of $\sim 3 - 15$ min and the lifetimes of the auroral structures are of the order of $2 - 10$ min (Sandholt et al., 1990).

If IMF $B_Z > 0$ and $B_Y > 0$, then the most probable merging region at the dayside magnetopause is in the duskside, but at higher latitudes than in the case of IMF $B_Z < 0$ and $B_Y > 0$ (Luhmann et al., 1984). When IMF $B_Z > 0$, the reconnection of the IMF and magnetospheric field lines poleward of the cusp may cause auroral activity in the polar cap region (Basinska et al., 1992).

Dusk sector auroral activity residing within the region of closed field lines cannot be directly related to dayside reconnection (Farrugia et al., 1994; Moen et al., 1994). At these latitudes, the plasma is convecting sunward and multiple arcs or transient spirals are typically observed when the solar wind speed is high, the IMF has a relatively strong radial component, and IMF B_Z is slightly positive. The auroras have been associated with R1 current enhancements as they are located just equatorward of the ionospheric convection reversal boundary. Mapping with empirical magnetic field

models have shown that their source region near the magnetic equator is $2 - 3 R_E$ inward from the magnetopause. Kelvin-Helmholtz waves developing at the inner edge of the low-latitude boundary layer (LLBL) is one of the most probable candidates to generate the auroras (Farrugia et al., 1994, 2000).

Auroral forms associated with magnetohydrodynamic wave activity can propagate polewards and anti-sunward and thus, greatly resemble FTE-type auroras (Milan et al., 1999). Nevertheless, the two-minute periodicity in the auroral emission indicates instead a connection to the wave activity rather than to dayside reconnection. In the study of Milan et al. (1999), ground magnetometer observations show pulsation activity, that is consistent with field line resonance eigenfrequencies and radar data shows that the wave activity also caused modulation of the ionospheric plasma drift velocity. The pulsating auroras at the open/closed field line boundary can be associated with modulations in the R1 current intensity. The boundary layer activity was coupled with inner magnetospheric processes as magnetic pulsations were recorded in an extended latitude range (MLATs 57–76).

Under suitable conditions, magnetopause surface waves triggered by solar wind pressure pulses can lead to magnetosheath plasma penetration into the magnetosphere (Woch and Lundin, 1992). Penetration events are observed within sunward convecting plasma during similar solar wind conditions as dusk sector arcs. Their occurrence rate increases when IMF $|B_X|$ is large and with increasing solar wind pressure. During dusk sector penetration events, IMF B_Y is preferentially positive, but the IMF B_Z direction does not con-

trol their occurrence significantly. Thus, these events could explain other than FTE-type auroras. However, the magnetosheath plasma injections flow systematically tailward, while for the cases analysed in the literature, the east-west motion of the auroras has not shown any preferred direction (Farrugia et al., 1994).

The so-called travelling convection vortices (TCV) (Glassmeier et al., 1989) are preferentially observed in the dawn sector, but in some cases, they can also cause auroral activity in the postnoon and dusk sectors. TCVs can be associated with field-aligned current (FAC) systems propagating dawnward and duskward away from noon. The FACs are conventionally assumed to have their source region at the magnetopause or in the LLBL, although recent studies (Yahnin and Moretto, 1996; Moretto and Yahnin, 1998) show that TCVs are typically observed in the region of central plasma sheet type precipitation. The current system includes both upward and downward directed currents which cause counterclockwise and clockwise directed Hall-current loops at their ionospheric footpoints (Glassmeier et al., 1989). As the current system propagates rapidly (a few km/s) anti-sunward, it is natural to assume that the related auroras also move in the same direction, although a case study by Lühr et al. (1996) comparing optical and magnetic observations show that auroras appear only occasionally at the footpoint of the upward FAC.

The aim of this study is to examine, with the combination of ground-based and Cluster observations, the role of magnetopause waves in the generation of the non-FTE type of dusk sector auroras. After a brief description of the instrumentation (Sect. 2), we present a comparison study of ground-based, Cluster II, and ACE observations made on 7 December 2000, during 13:30–15:30 UT (Sect. 3). Sections 4 and 5 summarize our findings with some discussion from the viewpoint of previous studies on dusk sector auroral activity.

2 Instrumentation

The Magnetometers – Ionospheric Radars – All-sky Cameras Large Experiment (MIRACLE) is a two-dimensional instrument network which consists of the IMAGE magnetometer network (Lühr et al., 1998), eight all-sky cameras and the STARE radar system (Syrjäso et al., 1998). These instruments in the Scandinavian sector cover an area from subauroral to polar cap latitudes over a longitude range of about two hours in local time. The sampling interval of the IMAGE magnetometer recordings is 10 s. The digital all-sky cameras (ASC) have three filters at wavelengths 557.7 nm, 630.0 nm, and 427.8 nm. Auroral intensities are measured in analog-to-digital units (ADUs) varying from 0 to 255. In the standard mode the imaging interval is 20 s for 557.7 nm and 60 s for 630.0 nm and for 427.8 nm. The field-of-view (FOV) of an ASC is a circular area with a diameter of ~ 600 km (at a 110 km altitude). The spatial resolution of an ASC image varies between less than a one km distance per pixel (near the zenith) to a few km per pixel (near horizon). In

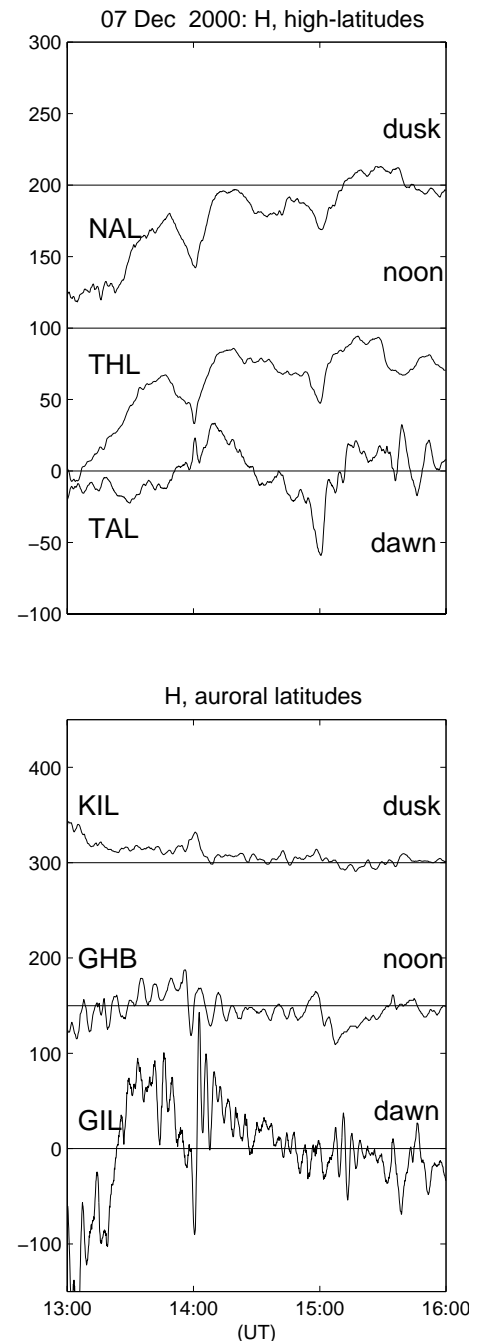


Fig. 2. Magnetograms (magnetic north component) from stations of IMAGE (NAL and KIL), CANOPUS (TAL and GIL) and Greenland (GHB and THL) networks.

this study, we use images acquired by the ITACA camera (Orsini et al., 2000) operating in Ny Ålesund (78.92° N and 11.93° E), Svalbard.

The CUTLASS (Co-operative UK Twin Located Auroral Sounding System) radar system consists of two HF radars and it is part of the international chain of SuperDARN radars (Greenwald et al., 1995). The CUTLASS radars are located in Hankasalmi, Finland (26.61° E, 62.32° N) and Pykkvibaer, Iceland (20.54° W, 63.77° N). The system provides high time

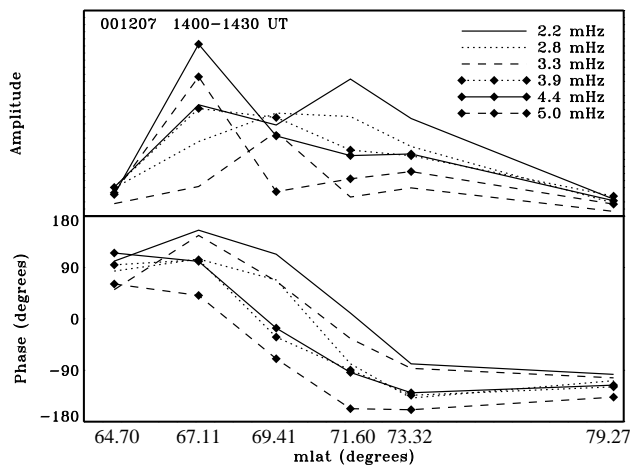


Fig. 3. Latitudinal variations of the Fourier amplitude and phases of the X-component along the CANOPUS Churchill line.

resolution measurements (120 s in routine operations) of the ionospheric flow vectors over an area of over 3 million km², with a line-of-sight resolution of the order of 50 km. The radar FOV is above northern Scandinavia and the Arctic Sea, covering also the Svalbard archipelago.

The Defense Meteorological Satellite Program (DMSP) is a set of sun-synchronous satellites in polar circular orbits at the altitude of ~ 835 km, and with an orbital period of ~ 100 min. Each DMSP satellite is instrumented with a complement of space environmental sensors. The DMSP auroral particle sensor, SSJ/4, measures the energy distribution of precipitating electrons and ions within the loss cone over the energy range from 32 eV to 30 keV (Hardy et al., 1984). The DMSP ionospheric plasma sensor, SSIES, measures the properties of the ionosphere including the convective motion of the background ionosphere (Rich, 1994). For the period of interest here, data from the DMSP F13 spacecraft during an overflight of Ny Ålesund is applicable to the discussion.

The ACE/MAG instrument measures the interplanetary magnetic field (IMF) vector near the Sun–Earth line at the upstream distance of $\sim 230 R_E$ from the Earth. The two magnetometers on ACE are wide-range tri-axial fluxgate magnetometers with a sampling rate of 1/30 s. In this study, we use data which has been averaged over 16 s. ACE/SWEPAM monitors the electron and ion fluxes in the energy ranges of 1–1240 eV and 0.26–35 keV, respectively. Below, we use dynamic pressure as determined from the ACE/SWEPAM proton density and speed observations (64 s averaged values).

During December 2000 and January 2001, the Cluster II spacecraft were still in the commission phase but their orbital plane was in the dusk sector and thus, the instruments gathered interesting data from the viewpoint of this study. On 7 December 2000, tests of the possible interference effects between the different types of instruments were performed. First tests of almost all instruments in operation were made during the period of the magnetic conjunction with the Svalbard region.

The Cluster Electric Field and Wave experiment (EFW) (Gustafsson et al., 1997) measures the electric field and the satellite potential with a high amplitude and time resolution. The experiment has four probes on wire booms in the spin plane of each satellite, with a probe-to-spacecraft separation of 44 m. The experiment is well suited to study both the large-scale structures (inter-spacecraft comparisons) and micro-scale structures (inter-probe comparisons). In this study, we use data of the satellite potential sampled at 5 samples/s. The satellite potential can be used to estimate the plasma density. Negative satellite potentials of -20 , -10 and -5 V correspond to plasma densities of about 0.9, 2 and 10 cm^{-3} (Pedersen et al., 2001).

The magnetic field instrument (FGM) (Balogh et al., 1997) on board each Cluster spacecraft consists of two tri-axial fluxgate magnetometers and a data processing unit. One of the magnetometers is located at the end of a 5.2 m long radial boom, and the other is at 1.5 m inboard from the end of the boom. Either of these sensors can be designed as the primary sensor which collects data with a higher time resolution than the other sensor. The instruments can measure the field with sampling rates of up to 67 vector/s. In this study, we use spin resolution (4 s) FGM measurements.

3 Observations on 7 December 2000

3.1 IMF, low-altitude satellite, and ground-based observations

According to Wind observations (satellite location $X_{GSE} \sim 40 R_E$, $Y_{GSE} \sim 170 R_E$, $Z_{GSE} \sim 8 R_E$) during 5 to 8 December 2000 the solar wind density was higher than that measured, during average conditions. A front of dense plasma was followed by high-speed streams (velocities around 600–700 km/s) during 8 to 12 December 2000. On 7 December, the solar wind density was $10\text{--}15 \text{ cm}^{-3}$ and the velocity was 420–460 km/s. Consequently, the dynamic pressure varied around 4 nPa (Fig. 8, third panel).

The IMF data (ACE/MAG data), together with IMAGE station Ny Ålesund (NAL) magnetograms, are shown in Fig. 1. The correlation between the ground magnetic north component (X) and IMF B_Z is best (0.7) when the delay from the ACE to dusk sector ionosphere is assumed to be 80 min. During 12:10–14:10 UT, ACE recorded primarily negative B_Y , with a short excursion to positive values around 12:50 UT. IMF B_Z and B_X varied between -5 and 8 nT. The solar wind proton density (data not shown) pulsed quasi-periodically around 13 cm^{-3} , with amplitudes up to 2 cm^{-3} . The dominant periods of the density pulsations are $\sim 8\text{--}9$ min, but short- and long-period pulsations are superposed. At the same time, the solar wind speed fluctuated with similar periods.

Figure 2 shows six H (magnetic north component) magnetograms of some IMAGE, Greenland network (Friis-Christensen et al., 1985) and CANOPUS (Rostoker et al., 1995) stations. The figure shows for each network data from

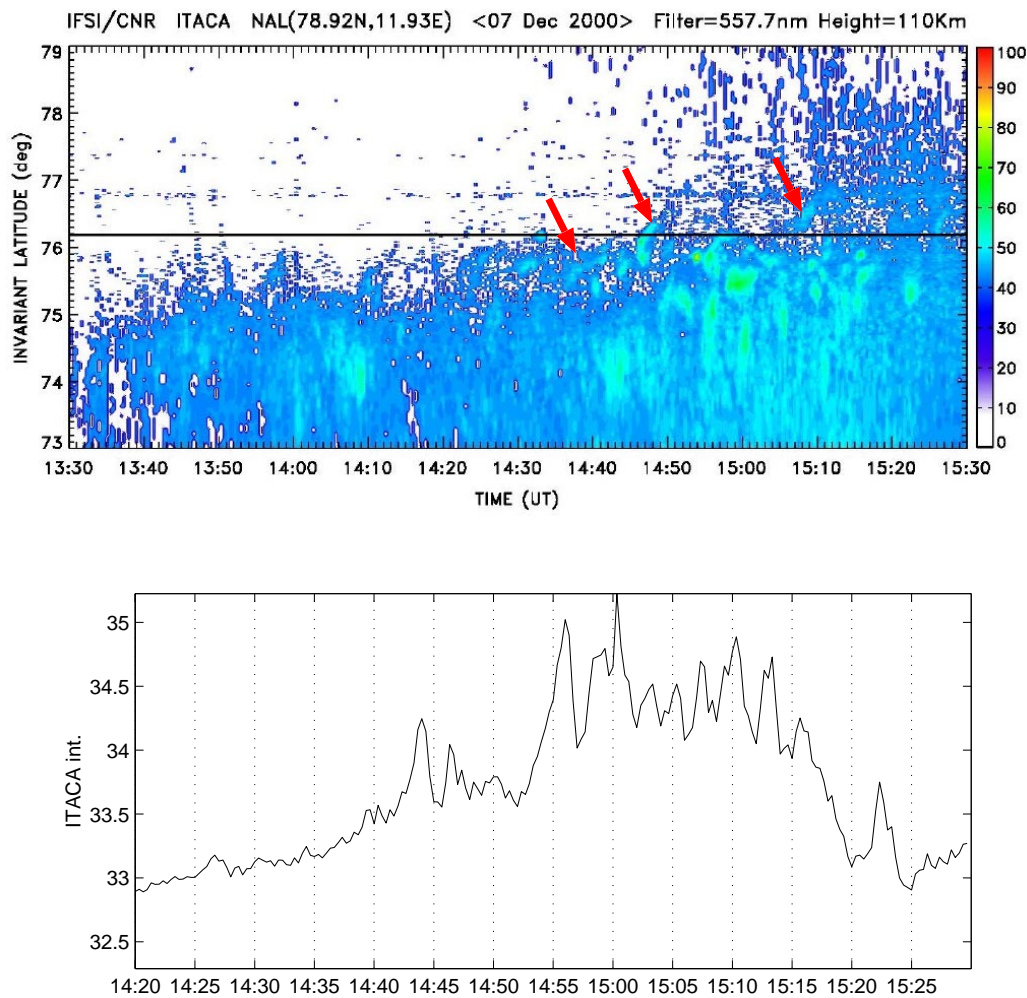


Fig. 4. (Top panel) The ITACA keogram and (bottom panel) temporal variations of the average auroral intensity (in ADUs) along the middle magnetic meridian of the camera FOV.

one high-latitude station (MLATs 76.1–85.7, AACGM coordinates are used throughout this study) and one station at standard oval latitudes (MLATS 65.9–70.9). When IMAGE was in the dusk sector, Greenland and CANOPUS magnetometers monitored the noon and dawn sectors, respectively. The magnetograms recorded at auroral latitudes show during the entire period pulsations in the Pc 5 range. The pulsations are evident in the noon and dawn sectors and somewhat weaker, but discernible in the dusk sector. The largest amplitudes were recorded at the CANOPUS stations after 14:00 UT. The large amplitudes can be related to the IMF B_z excursion to negative values, as observed by ACE at 12:40 UT (Fig. 1). This excursion temporarily enhanced the ionospheric convection which can be seen as negative (evening cell) and positive bays (morning cell) around $\sim 14:00$ UT in the H magnetograms of the high-latitude stations. Similar convection enhancement took place also around $\sim 15:00$ UT (IMF turning after 13:10 UT), although by then, the morning sector ionospheric convection reversal had moved to higher latitudes so that TAL was no longer monitoring the polar cap convection but rather the sunward

convection, which caused negative deviations in H .

The results of the Fourier-analysis of the X-pulsations observed during 14:00–14:30 UT by the Churchill meridional chain of CANOPUS stations (ISL, GIL, CHU, ESK, RAN, and TAL) are shown in Fig. 3. The plots show the Fourier amplitudes and relative phases at different frequencies as functions of latitude. The curves illustrate the characteristics typical for field line resonances (FLRs) (Chen and Hasegawa, 1974). The latitude of maximum amplitude decreases with increasing frequency. According to CANOPUS observations, the amplitudes of 5.0 and 4.4 mHz peak at GIL (MLAT 67.11°), that of 3.3 mHz at CHU (MLAT 69.41°), and the amplitude of 2.2 mHz at ESK (MLAT 71.6°). At frequencies 2.8 and 3.9 mHz, the peaks in the amplitudes are less pronounced. For all frequencies, the phases decrease with $\sim 180^\circ$ at the latitudes of maximum amplitude, which also is a typical FLR feature.

Figure 4 shows the ITACA keogram (intensity versus latitude along the middle magnetic meridian of the camera FOV) for the period of 13:30–15:30 UT. After 13:25 UT, the all-sky camera (MLAT = 76.1, MLT \sim UT + 3) started to observe

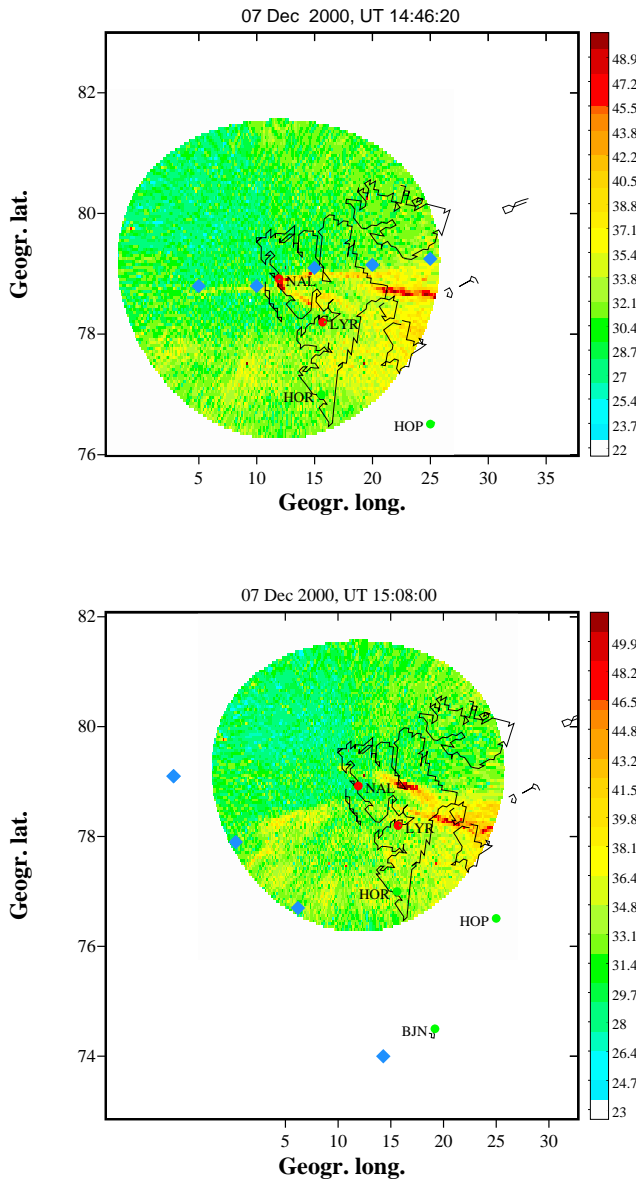


Fig. 5. Mapped ASC images (wavelength 557.7 nm, intensity in ADUs) recorded by ITACA at Ny Ålesund at 14:46:20, and 15:08:00 UT. The altitude of the auroras is assumed to be 110 km. The diamonds in the upper plot delineate the poleward edge of the auroras and in the lower plot they show the DMSP F13 footpoints during 15:06–15:08 UT (Fig. 5). In the lower plot, the second diamond from the top marks the poleward edge of the auroral precipitation observed by DMSP.

faint auroras near the southern horizon. The auroras stayed in the horizon until $\sim 13:47$ UT when the auroras also appeared in the southern sky of Ny Ålesund. This auroral activation can be associated with the convection enhancement observed by the polar cap magnetometer stations, as both the auroras and convection ceased at $\sim 14:10$ UT. After 14:26 UT, the auroras reappeared near the zenith, and folds and rayed structures were observed until $\sim 15:20$ when clouds started to gradually disturb the recordings. Again, these auroras can be

associated with enhanced convection and the IMF B_z turning to negative values, although the auroras brightened somewhat earlier than when the IMF turning (with the 80 min delay) took place. Faint poleward propagating auroras (marked with the red arrows) near the zenith were observed between 14:40–15:15 UT. Sunward propagating structures are visible at least in the ITACA frames acquired at 14:45–14:47 UT and 15:21–15:22 UT. Examples of the ITACA frames (on maps) recorded during the latter period of enhanced activity are shown in Fig. 5.

The DMSP F13 satellite flew above the ITACA FOV during 15:03–15:11 UT. The track of the satellite footpoints is shown in the second frame of Fig. 5 and the particle precipitation data and electric field observations (as converted to plasma flow velocities) are shown in Fig. 6. The location of the poleward edge of the auroras (marked with the vertical line in Fig. 6) coincides with the poleward edges (at 15:07 UT) of structured electron precipitation and energetic ion precipitation. Furthermore, at the same latitudes, the satellite observed the evening sector ionospheric convection reversal, where the sunward convection (lower latitudes) changed to anti-sunward convection (higher latitudes).

3.2 Cluster II observations

Figure 7 shows the Cluster orbit and spacecraft configuration during 13:30–15:30 UT (the distances between the four spacecraft have been multiplied by 10 to show the configuration more clearly). According to EFW observations, the magnetopause was closer to the Earth than, for example, the statistical magnetopause model by Shue et al. (1997) suggests. Consequently, the spacecraft were primarily in the magnetosheath just outside the high-latitude dusk flank of the magnetopause or in the magnetospheric boundary layers, either in the high-latitude boundary layer (HLBL) or in the LLBL. Spacecraft 2 (Salsa) was about 800 km sunward from the other spacecraft.

Satellite potential recordings are available only from spacecraft 3 (Samba). The negative of the potential ($-\phi$) is shown in the second panel of Fig. 8. During the periods when Samba was in the dense magnetosheath plasma, $-\phi$ was around -4 V, while during the visits into the thinner magnetospheric plasma, $-\phi$ dropped down to values of < -10 V. The $-\phi$ values in the range of $-6 \dots -5$ V correspond to plasma densities around 10 cm^{-3} which is a typical magnetosheath or solar wind density, while the $-\phi$ values between $-10 \dots -15$ V correspond to magnetospheric plasma densities (1 cm^{-3}) (Pedersen et al., 2001).

During 13:40–14:10 UT, $-\phi$ exhibits several quasi-periodic ($T \sim 4\text{--}6$ min) transitions between magnetospheric and magnetosheath plasmas. During 14:10–14:25 UT, the satellite potential shows variations with shorter periods ($T \sim 1$ min) and smaller amplitudes. With $-\phi$ close to -5 V, this suggests that Samba stayed at the outer edge of the magnetopause or in a magnetospheric boundary layer during this period. A couple of encounters with magnetospheric-type plasma were recorded around 14:30 UT and 14:45 UT,

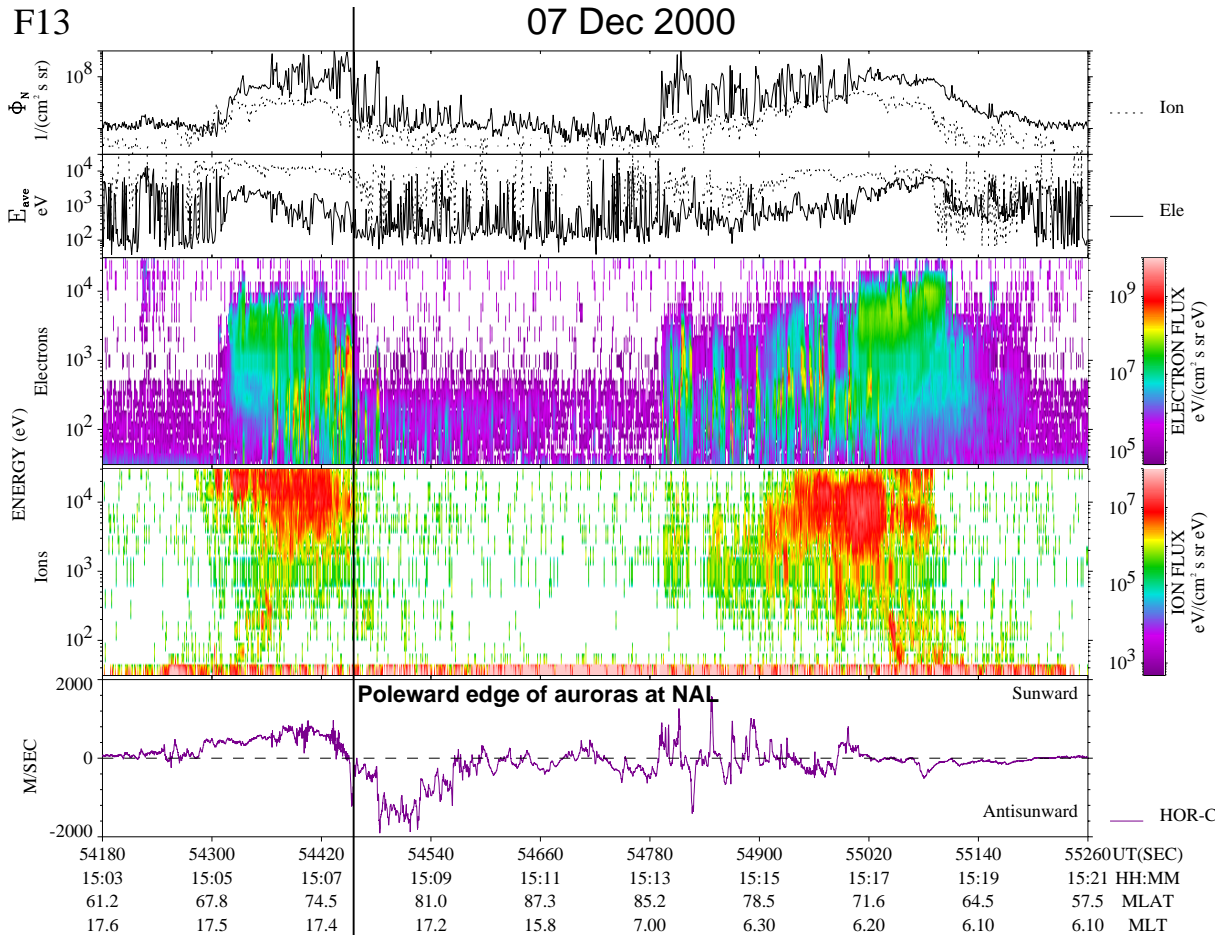


Fig. 6. Data recorded by DMSP F13 instruments during the track shown in Fig. 5 (from top to bottom): Ion and electron number fluxes and average energies, spectra showing differential energy fluxes, and plasma flow velocities. The vertical line marks the location of the poleward edge of the auroras shown in Fig. 5.

and after $\sim 14:50$ UT, the spacecraft eventually moved further away from the magnetopause.

The top panel of Fig. 8 is a reproduction of the third panel of Fig. 1 showing the IMF B_Z as recorded by ACE/MAG. Due to the differences in the signal propagation speeds along the magnetopause and into the ionosphere, the time delay of 80 min which gives the best correlation with the ground-based observations may not directly be applicable in the comparisons with the Cluster data. Nevertheless, it seems that the density variations with smaller amplitudes took place only during the period of IMF $B_Z > 0$, while the larger oscillations were observed when IMF B_Z was primarily negative. Note also that IMF B_Z had quasi-periodic variations with a shorter period ($T \sim 1$ min), especially during 14:05–14:20 UT (delayed time) and with a longer period, for example, during 13:30–14:05 UT. The periods of the satellite potential variations follow surprisingly well the periods of the IMF B_Z oscillations. The bottom panel of Fig. 8 shows the dynamic pressure as derived from the ACE/SWEPAM 64 s resolution data. The longer period variations are visible also in this curve, especially during $\sim 13:45$ –14:10 UT.

The satellite potential oscillations can be associated with

certain magnetic field variations which were observed by the FGM instruments on board all four spacecraft. The signatures observed at Salsa systematically precede those observed at the other satellites. Thus, we can associate the variations with tailward propagating waves. Two examples of the magnetic variations associated with the waves, as recorded by the Salsa and Samba FGMs, are shown in Fig. 9. In order to resolve the real phase velocity of the waves along the magnetopause, the observed magnetic field vectors should be transformed to the LMN -coordinates (Russell and Elphic, 1979) (N normal to the boundary, M and L in the boundary tangential plane). For this case, defining the appropriate LMN -coordinates is difficult because data from a clear magnetopause crossing close enough to the time of interest are not available. Consequently, the phase velocities are estimated with the component along the Salsa-Samba line. The inter-spacecraft time delays are determined by visual comparison of the curves since both temporal variations and connecting signatures are mixed in the data and thus, the cross correlation method would not give reliable results. During the larger oscillations (period 13:40–14:10 UT), which we interpret as consequences of magnetopause surface waves, the

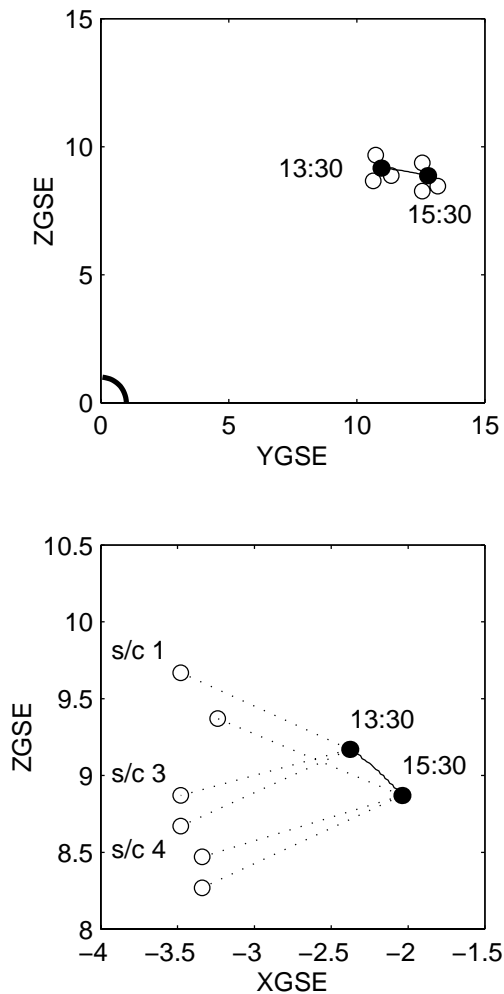


Fig. 7. Cluster orbit and configuration during 13:30–15:30 UT on 7 December 2000 in GSE YZ and XZ planes. The solid line and black dots show the location of spacecraft 2 (Salsa). In the bottom panel, the dashed lines join Salsa with the other spacecraft. For clarity reasons, the real inter-spacecraft distances have been multiplied by 10.

delays between the signatures observed at Salsa and Samba at the eight clearest transition times varied between 2 and 8 s (error in the timing ± 2 s), yielding estimates for the wave phase velocities in the range between 106 km/s and 385 km/s (± 100 km/s, average 215 km/s). The time delays associated with the shorter and smaller density pulsations (eight transition times) are significantly less scattered ($6\text{--}8$ s ± 2 s), yielding velocities 121–169 km/s (± 100 km/s, average 126 km/s).

4 Discussion

4.1 Solar wind MHD waves and magnetopause waves

The wave activity which Cluster observed at the magnetopause has a good correlation with the upstream solar wind variations recorded by ACE at $\sim 230 R_E$ (Fig. 8). A comparison of ACE/MAG and ACE/SWEPAM observations re-

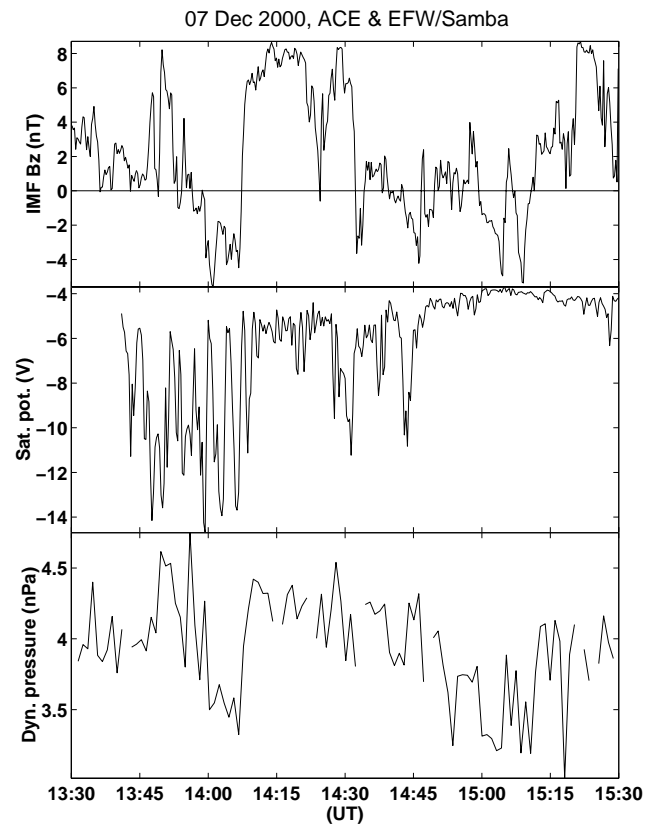


Fig. 8. (Top panel) IMF B_Z as recorded by ACE (time shifted by 80 min), (middle panel) negative of the satellite potential of Samba (spacecraft 3), and (bottom panel) dynamic pressure based on ACE/SWEPAM proton density and speed data.

veals that the corresponding components of the IMF and velocity are correlated, while the IMF magnitude is relatively constant. For a primarily positive IMF B_X , this suggests anti-sunward propagating Alfvén waves (Belcher and Davis, 1971) convecting at solar wind speed. However, since the solar wind proton density also pulsed quasi-periodically, the oscillations propagating in the solar wind were most likely a mixture of Alfvén and compressional waves.

The solar wind Alfvén waves interact with the bow shock, generating Alfvén and compressional modes in the magnetosheath (Lin et al., 1996; Sibeck et al., 1997). The MHD waves impinging on the magnetopause can cause pulsations in the reconnection rate and act as a source of Pc 5 pulsations in the magnetosphere (Lockwood et al., 2001; Prikryl et al., 1998). The compressional waves in the magnetosheath are expected to cause magnetopause surface waves, such as those observed by Cluster during the event discussed here. In addition, the fast mode is launched into the magnetosphere where it can couple to the shear mode driving the FLRs. In our case, magnetic field oscillations with periods in the range of 3–6 min were recorded, for example, by the geostationary GOES satellite in the dusk sector and by Geotail in the mid-tail ($X_{GSE} \sim -15 R_E$) midnight region (data not shown here). On the ground, FLRs cause magnetic pulsa-

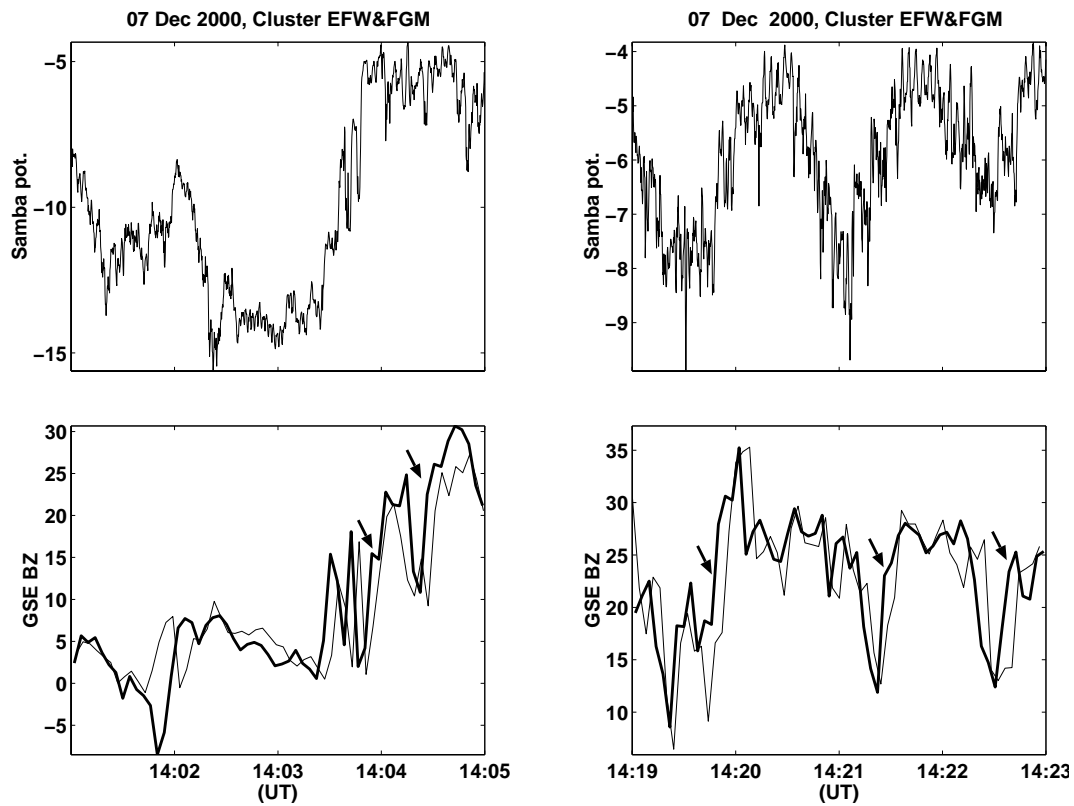


Fig. 9. Negative of the satellite potential of Samba and B_Z (GSE), as recorded by Salsa (thick line) and Samba (thin line) FGMs. Left (right) panel shows an example recorded during the larger (smaller) potential variations. The arrows point to the differences in the curves which have been used when estimating the phase velocities.

tions such as the magnetograms in our Fig. 2. Thus, a combination of Alfvén and compressional waves propagating in the solar wind was most likely one reason for the appearance of the magnetopause surface waves and magnetospheric and ground magnetic pulsations on 7 December 2000.

4.2 On the connection between surface waves and auroras

The theoretical study by Hasegawa (1976) shows that MHD surface waves can convert to kinetic Alfvén waves with an electric field component parallel to the background magnetic field. The parallel electric field can accelerate particles, for example, at the inner edge of the plasma sheet or the LLBL. Some observational support for the latter option is presented in the case study of high-latitude dusk sector auroras by Farrugia et al. (1994), although this study does not include any magnetospheric observations. The authors associate the waves with Kelvin-Helmholtz instabilities driven by the velocity and magnetic shears at the LLBL inner boundary. A more recent study by Farrugia et al. (2000) analysing in situ measurements from the equatorial magnetopause shows that the conditions for KHI to become unstable are more favourable at the LLBL inner boundary than at the magnetopause.

The solar wind conditions during our event are in many respects different from those events analysed by Farrugia et

al. (1994, 2000). In these events, the IMF B_Z stayed positive continuously and thus, energy transfer from the solar wind to the magnetosphere took place primarily via viscous interactions, while in our case, energy transport also took place via dayside reconnection during the periods of IMF $B_Z < 0$. In the case of Farrugia et al. (2000), abrupt changes in the solar wind density generated KH-type waves which propagated along the magnetopause from the noon to the flanks. Tailward propagating waves were also observed at the inner edge of the LLBL. In our case, the magnetopause fluctuations were at least partly driven by MHD waves in the solar wind. Despite these differences in the generation mechanisms, the waves described here and in Farrugia et al. (2000) have some similarities; in both cases, tailward propagating waves with periods in the Pc 5 range (accompanied by ground Pc 5 pulsations) were observed. Thus, it is reasonable to assume that from the viewpoint of the theory of Hasegawa (1976), in both cases, the waves should be able to generate auroras either within the sunward convecting field lines (LLBL inner edge waves) or at the convection reversal (magnetopause waves).

The magnetic field lines associated with the auroras analysed by Farrugia et al. (1994) map to the magnetospheric equatorial locations clearly inside the magnetopause, according to the model by Tsyganenko (1989). Similar mapping results for our event are presented in Fig. 10 which shows the location of the poleward edge of the auroras observed at

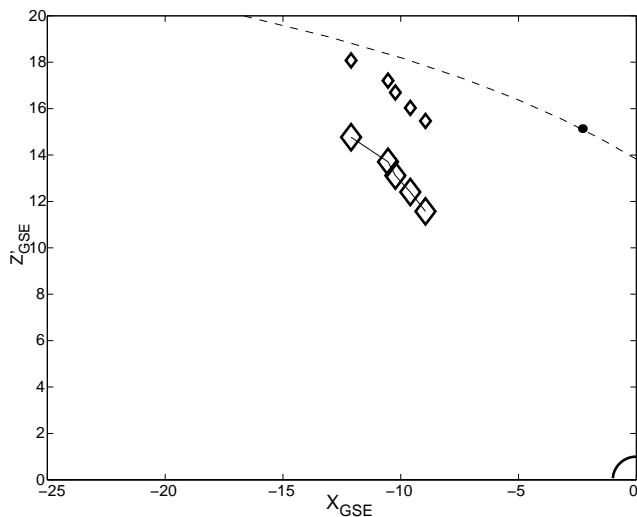


Fig. 10. The locations (the larger diamonds joined with the thin line) of the field lines conjugate with the poleward edge of auroras observed by ITACA at 14:46:20 UT (Fig. 5) in the plane defined by the Samba location and the X -axis of the GSE coordinate system. The dashed line shows the magnetopause location according to the model by Shue et al. (1997). The smaller diamonds show the maximum radial extents ($R = (Y_{\text{GSE}}^2 + Z_{\text{GSE}}^2)^{1/2}$) of the traced field lines.

the Ny Ålesund zenith at 14:46:20 UT (Fig. 5) mapped to the magnetic field model by Tsyganenko (1996) (hereafter referred as T96) to the plane where Samba was located at that moment. The spacecraft location is marked with the black dot and the dashed line shows the magnetopause location according to the model by Shue et al. (1997). The larger diamonds show the locations of the field lines in the plane of Samba, while the smaller diamonds show the largest radial extents of the field lines (achieved near the equatorial plane). Keeping in mind that in this case, the magnetopause was more contracted than the model suggests, we can conclude that the auroras had their source region near the magnetopause. The Cluster satellites were monitoring the magnetopause dynamics somewhat sunward from the conjugate region of the auroras, but not too far to make relevant comparisons with the ground-based observations.

From the basis of the mapping result of Fig. 10, we can assume that the auroras observed near the zenith of Ny Ålesund have their source region near the magnetopause surface waves observed by the Cluster spacecraft. These auroras can brighten either due to the magnetopause waves or due to R1 current enhancements associated with enhanced global convection driven by dayside reconnection. A nice correlation between variations in the convection and auroral emission in the R1 region is demonstrated in the study of Moen et al. (1995). The periods of the brightest aurora in the ITACA keogram of Fig. 4 roughly coincide with the IMF $B_Z < 0$ periods, although not exactly. It is evident, however, that the sign of IMF B_Z controls the appearance of the auroras rather than the existence of the magnetopause waves. Both ACE

and ground-based magnetometer observations (Fig. 2) show that the surface waves most likely persisted at the magnetopause during the whole UT afternoon.

Previously documented observations of ULF wave activity in the magnetospheric boundary layers (Farrugia et al., 2000) and in the R1 region of auroral precipitation (Milan et al., 1999) suggest that these phenomena would be mutually coupled and associated with Pc 5 pulsation activity at the auroral latitudes. Our data set supports this view, although the pulsations in the dusk sector ground-based observations are rather weak. At high-latitudes, magnetic pulsations were superposed with a longer period IMF B_Z controlled variations and thus, they were not as prominent as in the case of Milan et al. (1999). The intensities of the auroras were at times very low, but the time series of the average intensity along the middle magnetic meridian of the camera FOV (Fig. 4, bottom panel) has clear pulsations ($T \sim 2 - 3$ min) during 14:50–15:20 UT. During this same period, the ITACA keogram shows poleward moving structures which resemble the structures analysed by Milan et al. (1999), although in our case, the patterns are less regular.

4.3 Dawn-dusk asymmetry in the ground magnetic pulsations

Interestingly, Fig. 2 shows that there is a clear asymmetry in the pulsation characteristics observed on closed field lines on the ground between the dawn and dusk sectors. The dawn side waves (for example, at GIL) show the existence of large amplitude pulsations, while those at dusk are much less apparent and of a much lower amplitude. Observations from Cluster at the dusk side magnetopause show clear evidence of periodic magnetopause motion across the satellites, consistent with surface waves. Given that the magnetosheath flow is likely to be approximately symmetric down both flanks, one might ask why large amplitude pulsation activity is only observed on closed field lines at dawn.

One possible explanation involves the possibility that the magnetopause surface waves and pulsations on the ground are related to the development of the Kelvin-Helmholtz (KH) instability on the magnetopause or the low-latitude boundary layer. Recent work by Mann et al. (1999) has shown that in addition to the standard KH surface wave instability (Pu and Kivelson, 1983), it is also possible for the KH instability to inject energy into body modes which have a propagating character in the magnetosphere. Body type waves in the Pc 5 band on the flanks are usually associated with magnetospheric waveguide modes. These waveguide modes are trapped between the magnetopause and a turning point within the magnetosphere and hence, possess discrete frequencies, and propagate and disperse down the waveguide on the magnetospheric flanks (Walker et al., 1992; Wright, 1994).

The KH instability develops as a result of shear flow; however, the undulations that develop on the magnetopause can be stabilised by magnetic tension forces. As discussed by Lee and Olson (1980), the direction of the IMF would be expected to preferentially stabilise the dusk magnetopause

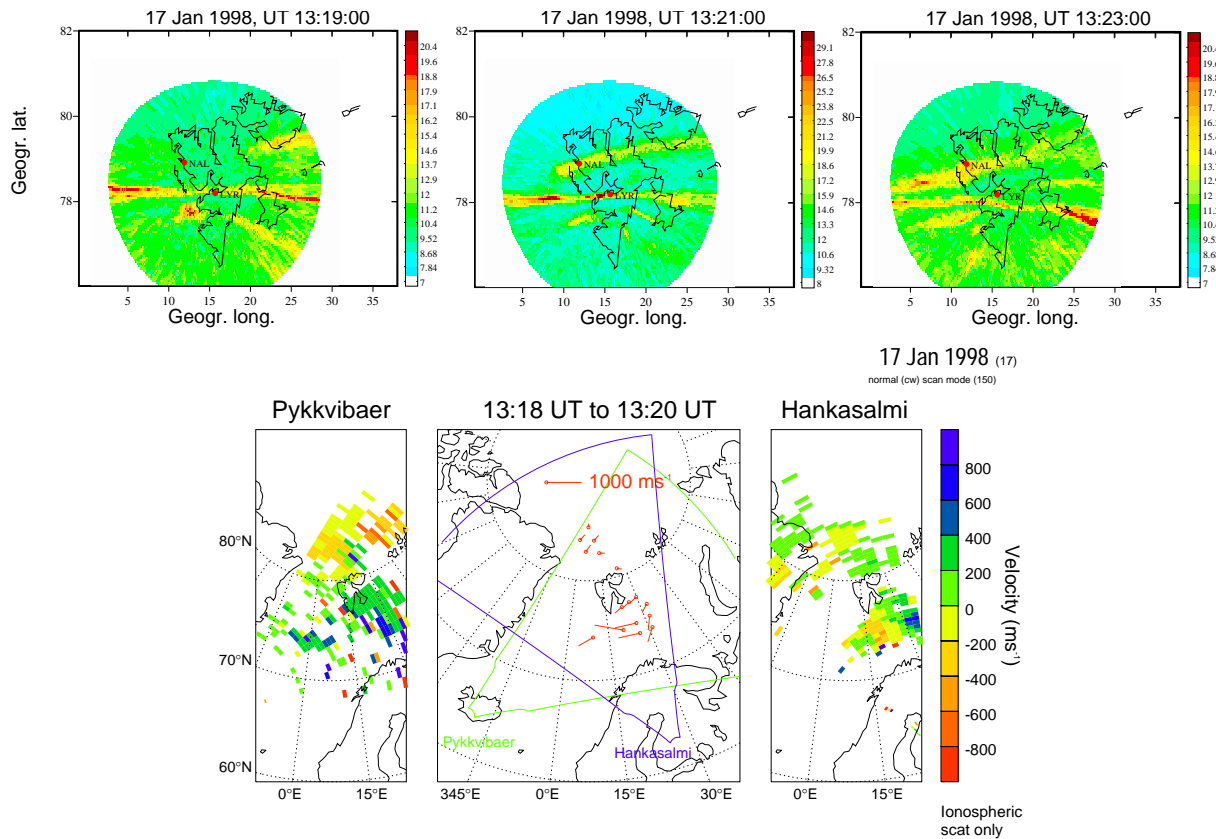


Fig. 11. Three ASC images (557.7 nm emission in ADUs, assumed to be at 110 km altitude) acquired at LYR on 17 January 1998, at 13:19, 13:20, and 13:23 UT and ionospheric plasma flow direction as observed by the CUTLASS radar system (plots in the bottom row). In the bottom row, the left (right) side plot shows the line-of-sight velocity of the Iceland (Finnish) radar. Positive velocities are towards the radar. The middle plot shows the actual velocity vectors as derived by combining the data of the two radars.

as compared to the dawn side. Moreover, as discussed by Mann et al. (1999), there is a critical magnetosheath flow speed which must be exceeded for body type magnetospheric modes to be energised by the KH instability, and this speed is, in general, larger than the critical speed required for the development of a KH surface wave. In the observations presented here (Fig. 3), the dawn side waves on closed field lines show some similarities with the amplitude and phase characteristics expected for waveguide mode driven field line resonances (Mathie et al., 1999). Moreover, as shown by Mathie and Mann (2000), the KH instability can be a very efficient driver of waveguide modes and hence, of large amplitude pulsations on closed field lines. Given that the dawn flank is likely to be more KH unstable than the dusk flank, it is possible that the criteria for the KH excitation of body waveguide modes was satisfied in the dawn sector, and resulted in the excitation of large amplitude pulsations on closed field lines. At dusk, however, where the KH is likely to be less unstable, it is possible that the criteria for the excitation of body waveguide modes by the KH instability was not satisfied. The dusk magnetopause could have remained KH unstable for the surface wave, with both Cluster and ITACA observing the consequences of this surface wave.

4.4 Sunward propagating auroral structures

If tailward propagating waves either at the magnetopause surface or at the inner edge of the LLBL are assumed to cause high-latitude auroral activity, there it is difficult to understand why sunward propagating brightenings occasionally appear in the auroras. On 7 December 2000, such brightenings were observed during two short (1–2 min) periods. In order to obtain a better view of how common sunward propagating brightenings are, we collected a reference data set of ASC images recorded in Svalbard during January 1998. The data set includes eight 1.5–3 h periods during which the ASC at LYR (MLAT = 75.2, MLON = 113.3, MLT \sim UT+3) observed dusk sector auroras. The set consists of 3720 ASC frames recorded with a 20 s resolution and a 557.7 nm filter.

Brightenings propagating sunward along the arcs are a relatively frequent and rather striking feature in the reference data set. In animations, the arcs seem to build up as “fingers” which intrude from the east horizon to the camera field-of-view. Such intrusions can appear either at the poleward edge of the auroral region or within the other arcs. One example of the former situation is shown in Fig. 11 with simultaneous plasma velocity recordings by the CUTLASS radar system. The arcs are in the region of sunward convecting plasma and

thus, the situation is similar to the studies by Moen et al. (1994) and Farrugia et al. (1994). According to Pykkvibær line-of-sight velocities, the sunward intruding arc resided close to the transition region between the sunward and anti-sunward flows. The average propagation speed of the “finger tip” of the arc is 2.6 km/sec, which is clearly higher than the surrounding plasma velocity. A similar event took place 15 min later, and according to simultaneous DMSP data, the arc in this case was just on the equatorward side of the polar cap boundary.

In summary, it seems that solar wind properties alone cannot control the appearance and dynamics of non-FTE type of dusk sector auroras. In addition, processes related to the sunward convecting return flow in the tail may modulate the dusk sector auroral precipitation. In the case of Fig. 11, however, quicklook plots of both AE index and geostationary particle fluxes as recorded by the Los Alamos National Laboratory instruments show quiet conditions in the tail around the time of interest.

5 Summary and conclusions

We have analysed high-latitude auroral activity and magnetopause dynamics in the dusk sector on 7 December 2000, from the basis of simultaneous ground-based and Cluster observations. A comparison of ACE upstream solar wind data and Cluster FGM and EFW data indicates a close connection between the magnetopause surface waves and quasi-periodic variations in the solar wind magnetic field, velocity and density. Wave modes with periods in the Pc5 range and around 1 min are most pronounced in the data, and comparisons of magnetic field observations of two Cluster spacecraft shows that the shorter and longer period waves were propagating tailward with mean velocities of 126 km/s and 215 km/sec, respectively. The solar wind MHD waves may not have been the only driver of the magnetopause waves. The apparent dawn-dusk asymmetry in the ground magnetic pulsation amplitudes suggests that also KHI developing at the magnetospheric boundary layers generated wave activity with different penetration depths in the dusk and dawn flanks.

We concentrated the analysis on the relationship between the magnetopause waves and auroras at the ionospheric convection reversal. Previous studies have shown that during extended periods of relatively constant IMF conditions (IMF $B_z > 0$), KH waves at the inner edge of the LLBL can cause high-latitude auroras (Farrugia et al., 1994, 2000) within sunward convecting field lines. We studied whether the same mechanism would also operate during more variable IMF conditions. According to Cluster observations, the properties of the waves in our case are in many respects similar to those observed by the spacecraft used in the study by Farrugia et al. (2000). It appeared, however, that the occurrence of the high-latitude auroras was controlled by the IMF B_z direction rather than by the surface wave activity. Visible auroras were observed preferentially during periods of IMF $B_z < 0$, when dayside reconnection enhanced the ionospheric con-

vection and R1 currents. During a short period we observed ~ 2 min pulsations in the auroral intensities, similar to the case study by Milan et al. (1999).

A wider inspection of the images acquired by the MIRACLE high-latitude ASCs revealed that sunward propagating brightenings are a relatively common feature in the dusk sector non-FTE type of auroras. A more detailed analysis of the magnetospheric and solar wind conditions favoring such behavior is needed in order to resolve whether the brightenings are associated with boundary wave dynamics, acceleration region phenomena, or with some magnetotail processes. Data collected during Cluster near-perigee conjunctions with the versatile ground-based instrument networks will be of great value also in such studies.

Acknowledgement. We thank the CDAWeb team, K. Ogilvie, H. Singer, and S. Kokubun for providing the possibility to check Wind, GOES and Geotail data from CDAWeb. ACE/SWEPAM data (PI D. J. McComas) was copied from the ACE Science Center web-page. Cluster spacecraft locations were defined with the help of OVT. The MIRACLE network is operated as an international collaboration under the leadership of the Finnish Meteorological Institute. The IMAGE magnetometer data are collected as a Finnish-German-Norwegian-Polish-Russian-Swedish project. IRF-U and CNR-IFSI participate to the data distribution and maintenance of the all-sky cameras. The CANOPUS program is a project of Canadian Space Agency and the Greenland magnetometer network is maintained by the Danish Meteorological Institute.

Topical Editor M. Lester thanks S. Milan and J. Moen for their help in evaluating this paper.

References

- Balogh, A., Dunlop, M. W., Cowley, S. W. H., Southwood, D. J., Thomlinson, J. G., Glassmeier, K. H., Musmann, G., Lühr, H., Buchert, S., Acuña, M. H., Fairfield, D. H., Slavin, J. A., Riedler, W., Schwingenschuh, K., and Kivelson, M. G.: The Cluster magnetic field investigation, *Space Sci. Rev.*, 79, 1/2, 65–91, 1997.
- Basinska, E. M., Burke, W. J., Maynard, N. C., Hughes, W. J., Winningham, J. D., and Hanson, W. B.: Small-scale electrodynamic activity of the cusp with northward interplanetary magnetic field, *J. Geophys. Res.*, 97, 6369–6379, 1992.
- Belcher, J. W. and Davis, Jr., L.: Large-amplitude Alfvén waves in the interplanetary medium, 2, *J. Geophys. Res.*, 76, 3534–3563, 1971.
- Chen, L. and Hasegawa, A.: A theory of long-period magnetic pulsations, 1, Steady state excitation of field line resonance, *J. Geophys. Res.*, 79, 1024–1032, 1974.
- Cowley, S. W. H., Morelli, J. B., and Lockwood, M.: Dependence of convective flows and particle precipitation in the high-latitude dayside ionosphere on the X and Y components of the interplanetary magnetic field, *J. Geophys. Res.*, 96, 5557–5564, 1991.
- Farrugia, C. J., Sandholt, P. E., and Burlaga, L. F.: Auroral activity associated with Kelvin-Helmholtz instability at the inner edge of the low-latitude boundary layer, *J. Geophys. Res.*, 99, 19403–19411, 1994.
- Farrugia, C. J., Gratton, F. T., Contin, J., Cochechi, C. C., Arnoldy, R. L., Ogilvie, K. W., Lepping, R. P., Zastenker, G. N., Nozdachev, M. N., Fedorov, A., Sauvaud, J.-A., Steinberg, J. T., and Rostoker, G.: Coordinated Wind, Interball/tail, and ground ob-

- servations of Kelvin-Helmholtz waves at the near-tail, equatorial magnetopause at dusk: 11 January 1997, *J. Geophys. Res.*, 105, 7639–7667, 2000.
- Friis-Christensen, E., Kamide, Y., Richmond, A. D., and Matsushita, S.: Interplanetary magnetic field control of high-latitude electric fields and currents determined from Greenland magnetometer data, *J. Geophys. Res.*, 90, 1325–1338, 1985.
- Glassmeier, K.-H., Hönisch, M., and Untiedt, J.: Ground-based and satellite observations of travelling magnetospheric convection twin vortices, *J. Geophys. Res.*, 94, 2520–2528, 1989.
- Greenwald, R. A., Baker, K. B., Dudeny, J. R., Pinnock, M., Jones, T. B., Thomas, E. C., Villain, J.-P., Cerisier, J.-C., Senior, C., Hanuise, C., Hunsucker, R. D., Sofko, G., Koehler, J., Nielsen, E., Pellinen, R., Walker, A. D. M., Sato, N., and Yamagishi, H.: Darn/Superdarn: a global view of the dynamics of high-latitude convection, *Space Science Reviews*, 71, 761–796, 1995.
- Gustafsson, G., Boström, R., Holmgren, G., Lundgren, A., Stasiewicz, K., Åhlén, L., Mozer, F. S., Pankow, D., Harvey, P., Berg, P., Ulrich, R., Pedersen, A., Schmidt, R., Butler, A., Fransen, A. W. C., Klinge, D., Thomsen, M., Fälthammar, C.-G., Lindqvist, P.-A., Christensson, S., Holtet, J., Lybekk, B., Sten, T. A., Tanskanen, P., Lappalainen, K., and Wygant, J.: The electric field and wave experiment for the Cluster mission, *Space Sci. Rev.*, 79(1–2), 137–156, 1997.
- Hardy, D. A., Smith, L. K., Gussenhoven, M. S., Marshall, F. J., Yeh, H. C., Shumaker, T. L., Hube, A., and Pantazis, J.: Precipitating electron and ion detectors (SSJ/4) for the block 5D/flights 6–10 DMSP satellites: Calibration and data presentation, Rep. AFGL-TR-84-0317, Air Force Geophys. Lab., Hanscom Air Force Base, Mass., 1984.
- Hasegawa, A.: Particle acceleration by MHD surface wave and formation of aurora, *J. Geophys. Res.*, 81, 5083–5090, 1976.
- Lee, L. C. and Olson, J. V.: Kelvin-Helmholtz instability and the variation of geomagnetic pulsation activity, *Geophys. Res. Lett.*, 7, 777–780, 1980.
- Lin, Y., Lee, L. C., and Yan, M.: Generation of dynamic pressure pulses downstream of the bow shock by variations in the interplanetary magnetic field orientation, *J. Geophys. Res.*, 101, 479–493, 1996.
- Lockwood, M., Cowley, S. W. H., and Onsager, T. G.: Ion acceleration at both the interior and exterior Alfvén waves associated with the magnetopause reconnection site: Signatures in cusp precipitation, *J. Geophys. Res.*, 101, 21 501–21 513, 1996.
- Lockwood, M., Opgenoorth, H., van Eyken, A. P., et al.: Coordinated Cluster, ground-based instrumentation and low-altitude satellite observations of transient poleward-moving events in the low and high altitude mantle regions, *Ann. Geophysicae*, this issue, 2001.
- Luhmann, J. G., Walker, R. J., Russell, C. T., Crooker, N. U., Spreiter, J. R., and Stahara, S. S.: Patterns of potential magnetic field merging sites on the dayside magnetopause, *J. Geophys. Res.*, 89, 1739–1742, 1984.
- Lühr, H., Lockwood, M., Sandholt, P. E., Hansen, T. L., and Moretto, T.: Multi-instrument ground-based observations of a travelling convection vortices event, *Ann. Geophysicae*, 14, 162–181, 1996.
- Lühr, H., Aylward, A., Bucher, S. C., Pajunpää, A., Pajunpää, K., Homböe, T., and Zaleski, S. M.: Westward moving dynamic substorm features observed with the IMAGE magnetometer network and other ground-based instruments, *Ann. Geophysicae*, 16, 425–440, 1998.
- Mann, I. R., Wright, A. N., Mills, K. J., and Nakariakov, V. M.: Excitation of magnetospheric waveguide modes by magnetosheath flows, *J. Geophys. Res.*, 104, 333–353, 1999.
- Mathie, R. A., Mann, I. R., Menk, F. W., and Orr, D.: Pc5 ULF pulsations associated with waveguide modes observed with the IMAGE magnetometer array, *J. Geophys. Res.*, 104, 7025–7036, 1999.
- Mathie, R. A. and Mann, I. R.: Observations of harmonic Pc5 field line resonance phase speeds: A diagnostic of their excitation mechanism, *J. Geophys. Res.*, 105, 10 713–10 728, 2000.
- McHenry, M. A. and Clauer, C. R.: Modeled ground magnetic signatures of flux transfer events, *J. Geophys. Res.*, 92, 11 231–11 240, 1987.
- Milan, S. E., Yeoman, T. K., Lester, M., Moen, J., and Sandholt, P. E.: Post-noon two-minute period pulsating aurora and their relationship to the dayside convection pattern, *Ann. Geophysicae*, 17, 877–891, 1999.
- Moen, J., Sandholt, P. E., Lockwood, M., Egeland, A., and Fukui, K.: Multiple, discrete arcs on sunward convecting field lines in the 14–15 MLT region, *J. Geophys. Res.*, 99, 6113–6123, 1994.
- Moen, J., Sandholt, P. E., Lockwood, M., Denig, W. F., Løvhaug, U. P., Lybekk, B., Egeland, A., Opsvik, D., and Friis-Christensen, E.: Events of enhanced convection and related dayside auroral activity, *J. Geophys. Res.*, 100, 23 917–23 934, 1995.
- Moen, J., Carlson, H. C., and Sandholt, P. E.: Continuous observation of cusp auroral dynamics in response to an IMF By polarity change, *Geophys. Res. Lett.*, 26, 1243–1246, 1999.
- Moretto, T. and Yahnin, A.: Mapping travelling convection vortex events with respect to energetic particle boundaries, *Ann. Geophysicae*, 16, 891–899, 1998.
- Newell, P. T., Feldstein, Y. I., Galperin, Y. I., and Meng, C.-I.: Morphology of nightside precipitation, *J. Geophys. Res.*, 101, 10 737–10 748, 1996.
- Newell, P. T., Burke, W. J., Meng, C.-I., Sanchez, E. R., and Greenspan, M. E.: Identification and observations of the plasma mantle at low altitudes, *J. Geophys. Res.*, 96, 35–45, 1991.
- Opgenoorth, H. J., Lockwood, M., Alcaydé, D., et al.: Coordinated Ground-based and Cluster observations on global and local scales, during a transient postnoon sector excursion of the dayside magnetospheric Cusp in response to solar wind variations, *Ann. Geophysicae*, this issue, 2001.
- Orsini, S., Kauristie, K., Massetti, S., Cerulli-Irelli, P., Candidi, M., Syrjäso, M., Baldetti, P., Morbidini, A., Sparapani, R., and Tabacchioni, F.: A new all-sky camera – ITACA – is part of the MIRACLE network, Proc. 5th International Conference on Substorms, St. Petersburg, Russia, 16–20 May 2000, ESA SP-443, ESA Publications Division, ESTEC, Noordwijk, The Netherlands, 2000.
- Pedersen, A., Décréau, P., Escoubet, C.-P., Gustafsson, G., Laakso, H., Lindqvist, P.-A., Lybekk, B., Mozer, F., and Vaivads, A.: Cluster four-point high time resolution information on electron densities, *Ann. Geophysicae*, this issue, 2001.
- Prikryl, P., Greenwald, R. A., Sofko, G. J., Villain, J. P., Ziesolleck, C. W. S., and Friis-Christensen, E.: Solar-wind driven pulsed magnetic reconnection at the dayside magnetopause, Pc5 compressional oscillations, and field line resonances, *J. Geophys. Res.*, 103, 17 307–17 322, 1998.
- Provan, G., Yeoman, T. K., and Milan, S. E.: CUTLASS Finland radar observations of the ionospheric signatures of flux transfer events and resulting plasma flows, *Ann. Geophysicae*, 16, 1411–1422, 1998.
- Pu, Z. Y. and Kivelson, M. G.: Kelvin-Helmholtz instability at the magnetopause: Solution for compressible plasmas, *J. Geophys.*

- Res., 88, 841–852, 1983.
- Rich, F. J.: Technical Description for the Topside Ionospheric Plasma Monitor (SSIES, SSIES-2 AND SSIES-3) on Spacecraft of the Defense Meteorological Satellite Program (DMSP), Rep. PL-TR-94-2187, Air Force Phillips Laboratory, Hanscom Air Force Base, Mass., 1994.
- Rostoker, G., Samson, J. C., Creutzberg, F., Hughes, T. J., McDiarmid, D. R., McNamara, A. G., Vallance Jones, A., Wallis, D. D., and Cogger, L. L.: CANOPUS – A ground based instrument array for remote sensing the high-latitude ionosphere during the ISTEP/GGS program, *Space Sci. Rev.*, 71, 743–760, 1995.
- Russell, C. T. and Elphic, R. C.: ISEE observations of flux transfer events at the dayside magnetopause, *Geophys. Res. Lett.*, 6, 33–36, 1979.
- Sandholt, P. E., Lockwood, M., Oguti, T., Cowley, S. W. H., Freeman, K. S. C., Lybekk, B., Egeland, A., and Willis, D. M.: Mid-day auroral breakup events and related energy and momentum transfer from the magnetosheath, *J. Geophys. Res.*, 95, 1039–1060, 1990.
- Shue, J.-H., Cao, J. K., Fu, H. C., Russell, C. T., Song, P., Khurana, K. K., and Singer, H. J.: A new functional form to study the solar wind control of the magnetopause size and shape, *J. Geophys. Res.*, 102, 9497–9511, 1997.
- Sibeck, D. G., Takahashi, K., Kokubun, S., Mukai, T., Ogilvie, K. W., and Szabo, A.: A case study of oppositely propagating Alfvénic fluctuations in the solar wind and magnetosheath, *Geophys. Res. Lett.*, 24, 3133–3136, 1997.
- Syrjäso, M. T., Pulkkinen, T. I., Janhunen, P., Viljanen, A., Pellinen, R. J., Kauristie, K., Opgenoorth, H. J., Wallman, S., Eglitis, P., Karlsson, P., Amm, O., Nielsen, E., and Thomas, C.: Observations of substorm electrodynamic using the MIRACLE network, in: Substorms-4, (Eds) Kokubun, S. and Kamide, Y., Proc. International Conference on Substorms-4, Lake Hamana, Japan, Terra Scientific Publishing Company, Tokyo, 1998.
- Tsyganenko, N. A.: Magnetospheric magnetic field model with a warped tail current sheet, *Planet. Space Sci.*, 37, 5–20, 1989.
- Tsyganenko, N. A.: Modelling the Earth's magnetospheric magnetic field confined within a realistic magnetopause, *J. Geophys. Res.*, 100, 5599–5612, 1996.
- Walker, A. D. M., Ruohoniemi, J. M., Baker, K. B., and Greenwald, R. A.: Spatial and temporal behavior of ULF pulsations observed by the Goose Bay HF radar, *J. Geophys. Res.*, 97, 12 187–12 202, 1992.
- Woch, J. and Lundin, R.: Signatures of transient boundary layer processes observed with Viking, *J. Geophys. Res.*, 97, 1431–1447, 1992.
- Wright, A. N.: Dispersion and wave coupling in inhomogeneous MHD waveguides, *J. Geophys. Res.*, 99, 159–167, 1994.
- Yahnin, A. and Moretto, T.: Travelling convection vortices in the ionosphere map to the central plasma sheet, *Ann. Geophysicae*, 14, 1025–1031, 1996.